Computers in Biology and Medicine 44 (2014) 66–75

Contents lists available at ScienceDirect

Computers in Biology and Medicine

journal homepage: www.elsevier.com/locate/cbm

A correlation analysis-based detection and delineation of ECG characteristic events using template waveforms extracted by ensemble averaging of clustered heart cycles

M.R. Homaeinezhad [a,b], M. ErfanianMoshiri-Nejad [b], H. Naseri [a,b,*]

[a] Department of Mechanical Engineering, K. N. Toosi University of Technology, Tehran, Iran
[b] Mechatronic Mechanisms Laboratory, K. N. Toosi University of Technology, Tehran, Iran

ARTICLE INFO

Article history:
Received 17 June 2013
Accepted 26 October 2013

Keywords:
Electrocardiogram
Random walks noise
P-and T-wave delineation
P-wave absence detection
Unsupervised waveform extraction
Synthetic ECG
Computerized implementation

ABSTRACT

The goal of this study is to introduce a simple, standard and safe procedure to detect and to delineate P and T waves of the electrocardiogram (ECG) signal in real conditions. The proposed method consists of four major steps: (**1**) a secure QRS detection and delineation algorithm, (**2**) a pattern recognition algorithm designed for distinguishing various ECG clusters which take place between consecutive R-waves, (**3**) extracting template of the dominant events of each cluster waveform and (**4**) application of the correlation analysis in order to delineate automatically the P- and T-waves in noisy conditions. The performance characteristics of the proposed P and T detection–delineation algorithm are evaluated versus various ECG signals whose qualities are altered from the best to the worst cases based on the random-walk noise theory. Also, the method is applied to the MIT-BIH Arrhythmia and the QT databases for comparing some parts of its performance characteristics with a number of P and T detection–delineation algorithms.

The conducted evaluations indicate that in a signal with low quality value of about 0.6, the proposed method detects the P and T events with sensitivity Se=85% and positive predictive value of P+=89%, respectively. In addition, at the same quality, the average delineation errors associated with those ECG events are 45 and 63 ms, respectively. Stable delineation error, high detection accuracy and high noise tolerance were the most important aspects considered during development of the proposed method.

1. Introduction

The surface electrocardiogram (ECG) signal can be interpreted as the heart electrophysiological response which reflects the functioning performance of the heart. Because the blood pumping function of the heart is fulfilled during a sequential process, hence, one of the most important characteristics of the ECG signal is its cyclic behavior, [1]. However, by working the vagal nervous system as the sympathetic and parasympathetic rate-regulation activities, the cyclic behavior of the ECG signal should be categorized as a cyclic random process with some associated characteristic specifications. The normal ECG signal is a train of successively occurring waves called as P (atrial depolarization), QRS (ventricular depolarization) and T (ventricular repolarization) waves [2]. Since each wave of the ECG signal reflects a specific physiological performance of the heart system, therefore cumulative analysis of all waves can generate some diagnosis about the health or abnormality of the heart function such as assessment of ventricular arrhythmia [3] and sudden death risk [4,5]. Thanks to the computational capabilities which computers of the present time provide, many complicated diagnosis and prognosis tasks can be carried out successfully which leads to promote the accuracy of health actions. Obviously, one of the most important steps of the computerized analysis of the ECG signal is the high-precision detection and recognition of the P and T events with enough stamina against noise and disturbing potentials. By referring to the knowledge databases, many studies are found for the detection of P- and T-waves such as application of the Phasor transform [6], slope estimation [7–9], mathematical modeling of P and T [10], multi-resolution wavelet analysis [11–16], support vector machine [17], and ensemble averaging [18]. These frameworks have been improved significantly in order to achieve a higher accuracy in P- and T-wave detection. However, a fully comprehensive technique which is capable to deal with all kinds of morphologies of P- and T-waves in noisy conditions is still needed. Moreover, in the reported researches, up to now, some problems exist which can be listed as follows:

- high computational complexity,
- high sensitivity to noise,
- heavy dependency on embedded thresholds,

* Corresponding author at: Faculty of Mechanical Engineering, K. N. Toosi University of Technology, P.O Box 19395-1999, Tehran, Iran. Tel.: +98 21 8406 3331, mobile: +98 9127502579; fax: +98 21 8867 7274.
E-mail address: hnaseri@gmx.com (H. Naseri).

0010-4825/$ - see front matter © 2013 Elsevier Ltd. All rights reserved.
http://dx.doi.org/10.1016/j.compbiomed.2013.10.024

- semi-automatic nature of some proposed algorithms which makes them dependent on existence of an expert user,
- not enough capability for recognizing and discriminating several waveforms,
- dependency on some train and a priori information about the P- and T-waves' features,
- and, significant delineation error associated with some conventional cases.

The aim of this article is to propose an algorithm for achieving the maximum possible accuracy of P- and T-wave detection and delineation process. In the present study, the cyclic nature of the cardiac system is resorted for finding P- and T-waves. This nature gives the opportunity to cluster the complete heart-beat cycles into some finite number of groups, in which the similarity between members of any group is significantly higher than the similarity between the members of different groups. By choosing this attitude for detecting the events of the ECG signal, the accuracy of the event detection algorithm is increased remarkably. In this study, by using a frequency-energy analysis, all ECG cycles are put into their appropriate clusters. Then, the template waveform of each cluster is calculated which will be used for abstraction of the P- and T-wave templates. By determination of the P- and T- wave templates, a search is conducted to find the signal segments with the highest similarity (correlation) relative to the P- and T- templates so as to be considered as the P- and T-waves. Moreover, in this article the relationship between signal quality value and the feasibility of extracting and delineating P- and T- waveforms has been explored. The concept of signal quality is a predominant subject which should be considered in real applications prior to application of a detection–delineation algorithm. In many previously published studies, this concept has not been considered particularly during statement of an algorithm total accuracy [19]. Intuitively, the performance of a designed ECG event detection algorithm does not remain identical in different noise levels i.e., it can be said that the performance of an algorithm should be assumed as a function of signal quality variable [19]. Hence, the stamina of a proposed algorithm should be reported as a part of total operating characteristics in order to give some statistics about the performance of the algorithm in real applications.

2. Materials and methods

The block diagram of the proposed method is demonstrated in Fig. 1.

2.1. Dataset

In this study, the performance of the proposed algorithm is verified by its implementation to several synthetic ECG signals with different qualities. The open source ECG simulation frameworks [20,21], were used to generate artificial ECG signals. Afterwards, the algorithm was evaluated using QTDB [22,23], and MITDB [24], in order to provide comparative results with existing algorithms.

By application of a synthetically generated ECG database, the operating characteristics of a detection–delineation algorithm can be given both qualitatively and quantitatively. First, by the synthetic ECG generation algorithms introduced by [20,21], the ECG signals with different waveforms and shapes such as normal, premature atrial or ventricular contractions, diverse infarctions, T-wave alternans and many other wave types can be generated. By implementation of the proposed ECG event detection algorithm to a database with different shapes, the accuracy of the algorithm versus waveshape variations is reported, (qualitative analysis). On the other hand, by combination of the synthetic ECG generation algorithm with the signal quality alteration technique proposed in Ref. [18], the accuracy of the algorithm both in detection and in location estimation of the events can be stated versus quality value of signal, (quantitative analysis).

2.2. Detecting ECG impulsive waves

The P- and T-waves detection algorithm introduced in this study requires the clustering of the complete heart cycles. For clustering the RR cycles, by applying a noise robust algorithm, the QRS complexes are detected. For detecting QRS complexes, in this study a probabilistic quantity called multiple higher-order moments (MHOM) [25] is used. By employing this feature, the low- and high-slope ECG events can be recognized. In summary, by applying the discrete wavelet transform (DWT), the dydic scale 2^4 is obtained. Then, a sliding window with the duration determined based on the sampling frequency is used for calculating the elements of the detection metric. Afterwards, the histogram analysis was applied to find comparison thresholds used for finding QRS boundaries. By delineating the QRS complexes, the signal segments located between successive R-waves are extracted and called as RR-cycles.

2.3. Detecting ECG non-impulsive waves (atrial depolarization and ventricular repolarization waves)

Even in the cases in which the arrhythmias and abnormalities occur, the heart's electrical performance can be clustered into some finite number of groups. In this way, several waveforms of the ECG signal can be divided into some dominant shapes. These shapes give a significant utility for detecting the exact place of an event as well as its onset and offset locations. To this end, the first step is to categorize the several cycle segments into some finite number of clusters. Next, by application of the ensemble averaging technique [1,26–28], the dominant pattern of each cluster is determined. If the number of cluster members is adequately large, the ensemble averaging technique will give a nearly noise-free waveform whose events can be detected straightforwardly. Reasonably, each cluster waveform includes its own events which might generate some information for more accurate diagnosis. Finally, for detection of P- or T-waves of each heart cycle, its mother cluster (the cluster which accepts that cycle as its own member) is determined. The waves of cycle are the segments that show the highest similarity (correlation) with the events of the holding cluster waveform. The noise robustness of this procedure is originated from the fact that the ensemble averaging technique compensates the effects of non-informative components of the original waveform which causes eventually an inherent filtering process, [1]. Thanks to the a priori information generated by determination of the cluster waveform, the detection of P- and T-waves is conducted with high accuracy. The detection of P, T or the absence of P without having their pattern at hand, will give unacceptable results in low-quality or abnormal ECG signals.

2.3.1. Clustering waveforms between two consecutive R-waves

In this step, the procedure for clustering the signal segments located between two successive R-waves is described. Although, the complete heart cycle is defined physiologically as the ECG segment which begins from the P-wave onset and ends to the T-wave offset, however because the event detected at the first trial is the QRS complex, the sequence of heart cycles is assumed as RS-T-P-QR instead of P-QRS-T. By this assumption, the complete heart cycle can be defined as the ECG segment located between two

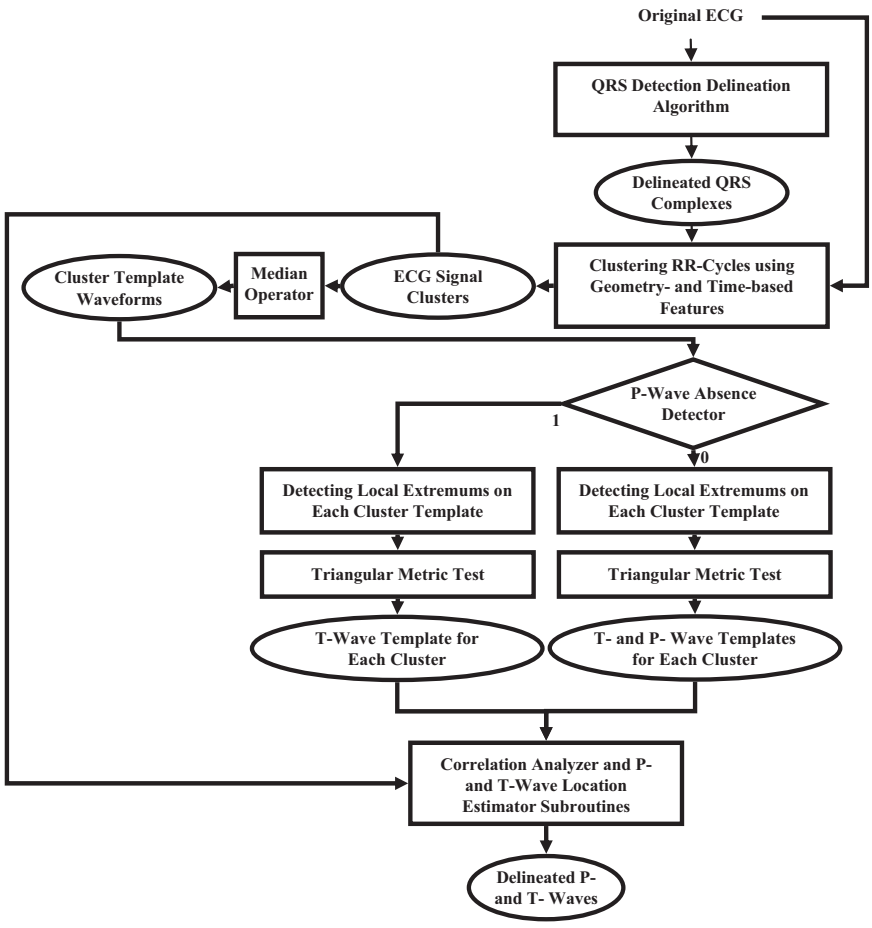

Fig. 1. The general block diagram of the proposed method for detecting and delineating ECG P-QRS-T events.

successive R waves. For clustering the heart cycles, the features are calculated based on the time duration and the geometry of cycles. In this article, clusters and cluster center waveforms are indicated by C_k and $C_k[n]$, respectively.

2.3.1.1. Cluster center waveform. Suppose that the ith cluster of the ECG signal contains n members. In order to determine the corresponding cluster waveform (or template waveform of the cluster), first the length of all members should be equalized. To this end, the mean value of the length of cluster members is calculated. Then, the length of all members is converted into this mean value by applying some simple interpolation and resampling techniques, [29]. Toward this objective, suppose that $\mathbf{f}_k$ is the array which contains the time-aligned samples of the kth member of the given cluster. The template waveform of the cluster is calculated by applying the ensemble averaging technique to all members of the cluster. That is

$$C_i[i] = \frac{\sum_{j=1}^{n} f_j[i]}{n} \tag{1}$$

2.3.1.2. Time comparison. Suppose that $RR_k[n]$ indicates the signal between the k-th and the $(k+1)$th R-waves whose length is indicated by RR_k. In order to compare RR cycles by time, first, the DC value of the sequence $RR_k[n]$ is removed. The obtained sequence called $RR_k^*[n]$ is chosen as the first cluster center ($C_1[n]$). Afterwards, other $RR_k[n]$s are compared one-by-one with the center of existing clusters. If RR_i indicates the length of the test cycle ($RR_i[n]$) and RR_{Mean} is the mean value of the sequence RR_k, the difference between RR_i and the length of $C_j[n]$ should not be more than $\tau_D = 0.1 \times RR_{Mean}$. If this condition is not satisfied, $RR_i[n]$ will not be included by the $C_j[n]$.

For calculation of the threshold τ_D, the signals of the MITDB are used. To this end, 1000 RR cycles are chosen from different ECG signals of the MITDB. The cycles are chosen from different ECG signals so as to include most of the cycle waveforms. During the selection of RR-cycles, it was tried to incorporate adequate number of all possible waveforms. Afterwards, the ECG cycles are clustered manually. For each cluster, the mean value of cycles duration is calculated. Then, the length of cycles is normalized by dividing the duration of each cycle length to the mean length of the cluster. By conducting the normalization procedure to all clusters, the distribution function of the normalized periods is computed. In Fig. 2, the distribution (histogram) of the normalized cycle durations is depicted. According to this histogram, it can be claimed that if the normalized duration of a test cycle is between 0.9 and 1, with the probability more than 99%, the given cycle belongs to the cluster whose length has been used for normalization of the test cycle length. Accordingly, the optimal value of the threshold τ_D is about 0.1. Empirical assessments show that the value $\tau_D = 0.1$ is suitable for a wide range of ECG signals with different qualities. In other words, the regulation of this threshold is not required when another database is used.

2.3.1.3. Geometric comparison. During the geometric comparison, the lengths of test cycle and cycle template must be equal. Depending to the fact that the cycle length of the cluster

members has some minor variations, the mean value of the cycle length of each cluster is calculated. Then, all cycles are mapped into this mean value by applying some simple interpolation and resampling techniques, [29]. Then, the DC value of the cycle $RR_i[n]$ is removed (indicated by $RR_i^*[n]$). Finally, the difference between $RR_i^*[n]$ and $C_j[n]$ (Fig. 3(a)) is calculated as

$$V_{RR}[n] = |RR_i^*[n] - C_j[n]| \tag{2}$$

In order to fulfill the cluster analysis of RR cycles, three conditions are examined:

- If the mean value of $V_{RR}[n]$ (indicated by V_{RR}) is greater than a threshold, the $RR_i[n]$ will not be included by the C_j. The value of the threshold is obtained from the following relationship:

$$\tau_R = 0.05 \times Min[Max[C_j[n]],\ Max[RR_i^*[n]]] \tag{3}$$

  where $Max[RR_i^*[n]]$ and $Max[C_j[n]]$ are the maximum value of the curves $RR_i^*[n]$ and $C_j[n]$, respectively.
- A second condition based on the deviation extent of $V_{RR}[n]$ from $\overline{V}_{RR}$ is assessed. As it is demonstrated in Fig. 3(b), if the difference of $\overline{V}_{RR}$ is greater than τ_V at least for τ_W samples, the $RR_i[n]$ will not be added to the tested cluster C_j. The thresholds τ_V and τ_W are calculated according to the following mathematical relationships:

$$\tau_W = 0.4 \times (2WL+1) \tag{4}$$

$$\tau_V = \frac{\overline{V}_{RR}}{2} + 2\left(\frac{\tau_R}{\overline{V}_{RR}}\right) - f(\overline{V}_{RR}) \tag{5}$$

  where

$$f(x) = \begin{cases} 0.3 \times \left(x - \frac{\tau_R}{2}\right) & x > \frac{\tau_R}{2} \\ 0 & x \le \frac{\tau_R}{2} \end{cases} \tag{6}$$

- Finally, the extent of discontinuous deviations of $V_{RR}[n]$ from $\overline{V}_{RR}$ should not exceed from a specific threshold. Otherwise, $RR_i[n]$ will not be included by C_j.

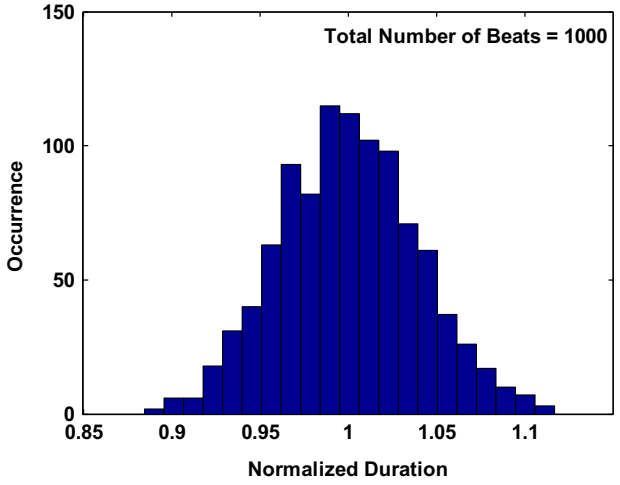

Fig. 2. The distribution (histogram) of the normalized cycles duration of all clusters for finding optimum τ_D.

The discriminating thresholds τ_R, τ_W, τ_V have been obtained based on the empirical assessments and trying-and-error tests conducted to several ECG cases. It should be noted that no further regulation of those thresholds is needed when another database is used.

If all conditions are validated, the test cycle is put into the cluster and the cluster center is updated by calculating the mean value of the old cluster center and the test cycle. Otherwise, the comparison is repeated with other existing cluster centers. In the cases in which the test cycle does not match with any existing cluster, that cycle is considered as the center of a new cluster. At the end of this stage, a correlation analysis is conducted between the centers of clusters. Those clusters with correlation coefficients more than 0.9, are merged with each other.

2.3.2. *Is the P-wave absent or is present?*

In order to decide on the existence of a P-wave on the cluster center waveform, the time duration of the longest cluster is taken as the scaling length, indicated by L. As a matter of fact, in order to use the longest cluster as the scaling length, there must be a cluster which includes at least 75% of the length of the longest cluster. Otherwise, the second longest cluster is chosen as the scaling length (L) and so forth. The P-wave is absent in a cluster whose length is less than 70% of L. In Fig. 4(b), the length of three sample clusters are compared with L.

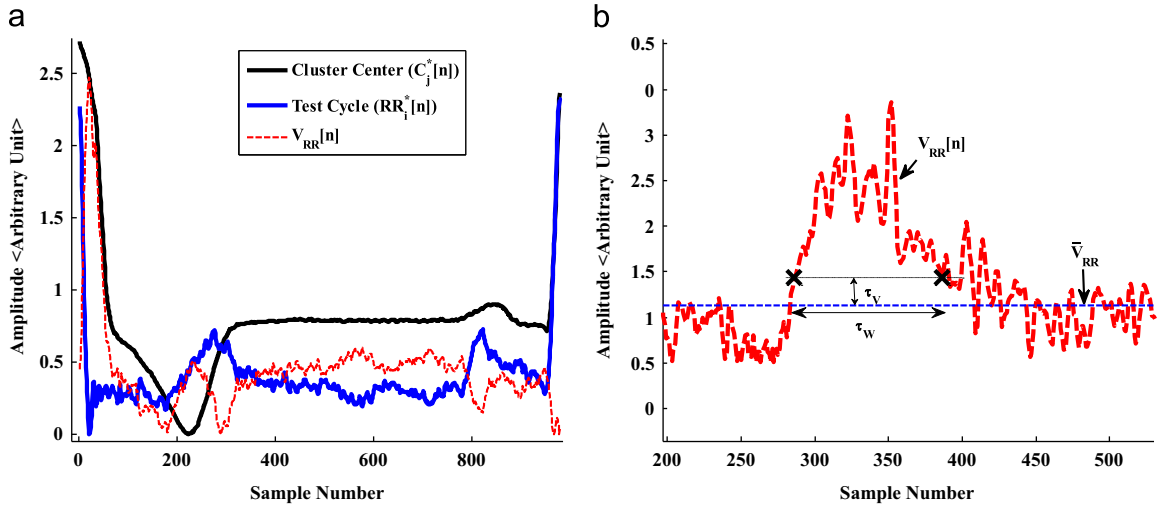

Fig. 3. (a) Simultaneous illustration of a cluster center waveform, test cycle and their difference ($V_{RR}[n]$) and (b) illustration of deviation of $V_{RR}[n]$ from its own mean value named as $\overline{V}_{RR}$.

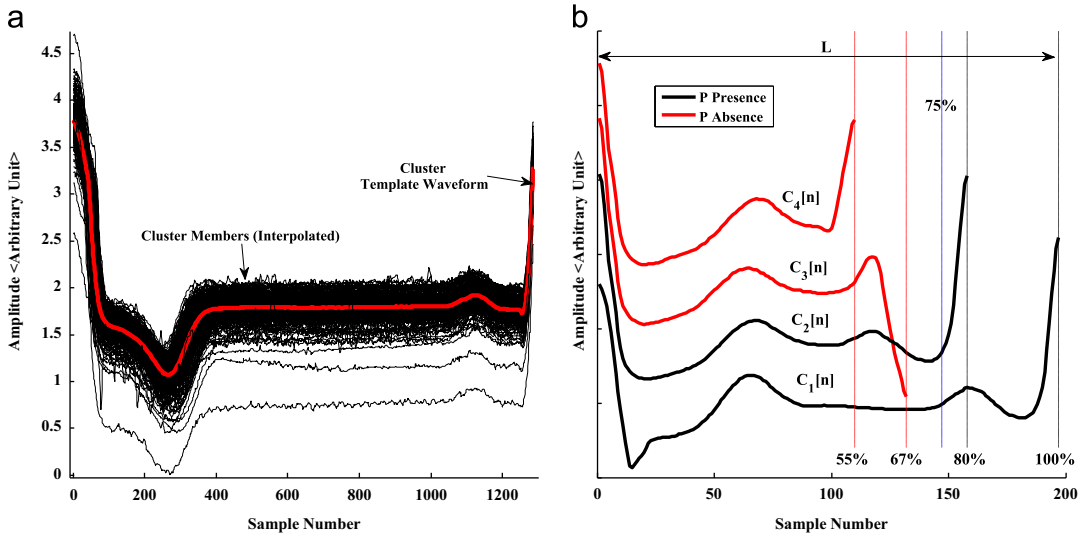

Fig. 4. (a) The members of a cluster which are similar from time and geometry points of view. The cluster waveform (cluster center) $C_i[n]$ is also illustrated, (b) deciding about the presence or absence of the P-wave by comparing the cycle length with the scale length (L).

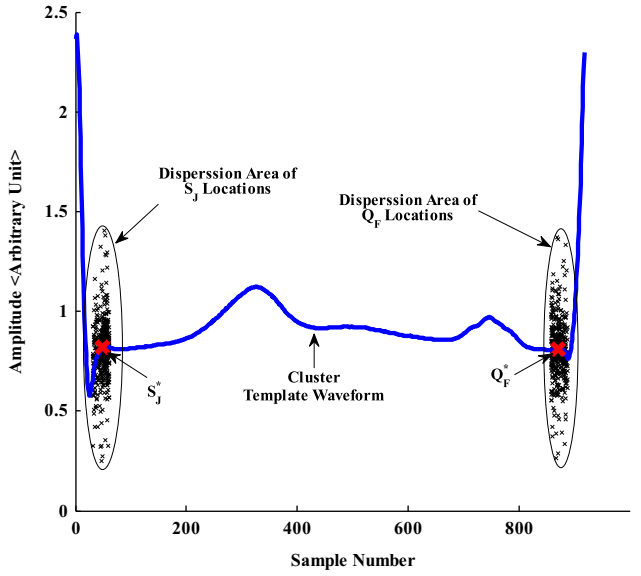

Fig. 5. Estimating the locations of S_J^* and Q_F^* of a cluster center waveform by analyzing the distributions of the cluster member S_J and Q_F locations.

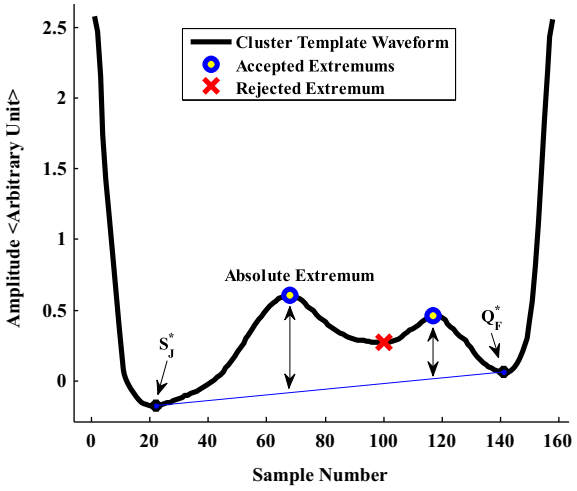

Fig. 6. The procedure of finding an absolute extremum of the cluster center waveform. Deletion of a local minimum which is in a higher position relative to locations of S_J^* and Q_F^*.

2.3.3. *Local extremums of cluster center waveform*

For identifying the events which occur in the waveform of each cluster, first, their local extremums are determined by applying the method introduced in Section 2.1. Then, for each cluster, by using the distribution of the members Q_F and S_J locations, the corresponding Q_F and S_J locations (indicated by Q_F^* and S_J^*, respectively) are determined for the cluster center, (Fig. 5).

The value of each local minimum must be less than the values of Q_F^* and S_J^* simultaneously. Otherwise, it is removed from the extremum population. Similarly, the value of a local maximum must be greater than the values of the Q_F^* and S_J^*. Otherwise, that local maximum will be removed from the extremum population, too, (Fig. 6). As it is demonstrated in Fig. 6, a straight line is drawn from S_J^* to Q_F^*. The extremum which has the longest distance from the line is called the absolute extremum which is certainly a real event (a P- or T-wave).

In many practical cases, it might be possible that a P-wave is not absent, but due to some reasons, an associated extremum cannot be found. In such situations, the only solution is to assign an interval in which the P-wave might be found with the highest probability.

2.3.4. *Determining the onset and offset of non-QRS waves*

In this section, it is assumed that each accepted local extremum is the center of a real P- or T-wave. By this assumption, an interval which shows the accurate boundary of the event, should be determined for each accepted extremum. To this end, a quantity called trigonometric curve is calculated and is indicated by $G[n]$:

$$G[n] = O(E_i^C, n) \times \tan(\theta_n), \quad S_J^* \le n \le Q_F^* \tag{7}$$

where E_i^C is the location of the i-th local extremum and $O(E_i^C, n)$ is the Euclidean norm between the local extremum E_i^C and the sample n. In addition, θ_n is the angle between the horizontal line and the line which connects the location of E_i^C to the location of the n-th sample.

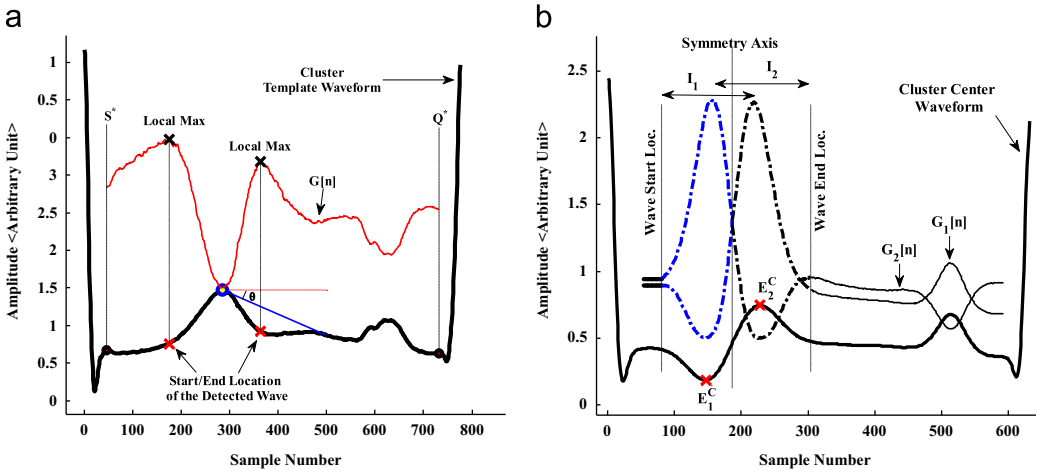

Fig. 7. (a) Finding the boundary of P or T on the cluster center waveform using the detection metric $G[n]$ and (b) calculation of $G[n]$s for two adjacent local extremums in order to determine the onset and offset of a biphasic wave.

In the vicinity of the extremum E_i^C located on the curve $G[n]$, two local maximums are seen (Fig. 7(a)). The locations of these maximums are the onset and offset of the event. If it can be concluded that the P-wave is absent, the event which has the maximum amplitude is determined as the T-wave which occurs certainly at the place of the absolute extremum. Otherwise, two events which have the highest amplitudes are extracted as the P- and T- waveforms. Certainly one of them is at the place of the absolute extremum.

2.3.5. Biphasic waves

Some of the P- or T-waves are biphasic. When a biphasic event occurs, two local extremums (a local maximum and a local minimum) are seen. In such cases, the $G[n]$ feature is calculated for both of these extremums. If $G_1[n]$ is calculated for the first extremum (E_1^C) and $G_2[n]$ is calculated for the second one (E_2^C), $G_1[n]$ and $G_2[n]$ are symmetric in the interval where the biphasic event occurs. In other words, the existence of two symmetric $G[n]$ curves for two adjacent local extremums implies that a biphasic wave exists on the cluster center waveform. Based on the assumption that E_1^C and E_2^C are the peaks of two events, their onsets and offsets are determined by $G_1[n]$ and $G_2[n]$, respectively. The segments associated with the E_1^C and E_2^C, are indicated by I_1 and I_2, (Fig. 7(b)). When a biphasic wave occurs, I_1 and I_2 are merged in order to form its occurrence interval. It should be noticed that this method is suitable for delineating P- or T-waves which are similar to the templates shown in Fig. 7. For finding all types of P- or T-waves, some other researches should be conducted so as to arrange the requirements and steps needed to detect and to delineate different waves.

2.3.6. Correlation analysis and location guess procedures

After determination of the P and T patterns, these templates are moved on a test cycle. During each sample forward movement of the calculated patterns, the similarity extent between the excerpted segment and each template is ranked according to the criterion introduced in [30,31]. By termination of the correlation analysis of the test segment, the window which has the highest fitness score versus the pattern waveform is determined as the event associated with the template signature.

To illustrate the definition of this score, suppose that the signal within the test window is indicated by x and the T- or P-wave template is indicated by $\hat{x}$. By subtracting the $\hat{x}$ from x, the residual sequence $\tilde{x}$ will be obtained from $\tilde{x}=\hat{x}-x$. Fitness score ρ depends upon the sum of the squares of the residuals normalized by the energy of the signal, [30,31]:

$$\rho = max\left(1-\sum\frac{\tilde{x}^2}{\sum x^2 - mean(x)^2},0\right) \quad (8)$$

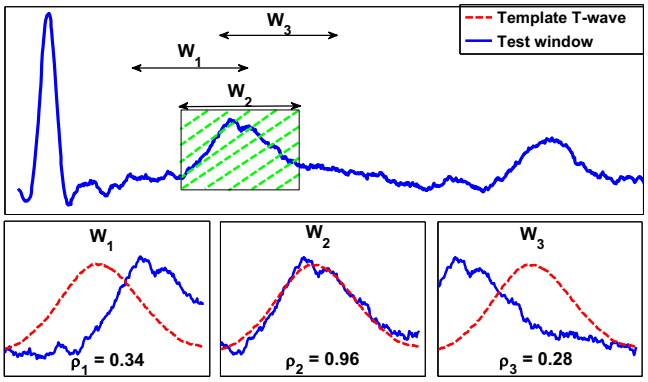

Fig. 8. Correlation based detection–delineation of T-wave.

In Fig. 8, the graphical illustration of T-wave detection procedure is depicted. In three windows indicated by W_1, W_2, and W_3, the waveform of cycle and the template T-wave are compared. Because of the fact that ρ_2 is the greatest value among other ρ's, the W_2 is chosen as the location of T-wave.

Upon finishing the cluster analysis phase described in Section 2.3, some clusters with only one member (called isolated clusters) might appear. For identifying P- or T-waves in such clusters, the templates obtained from high population clusters are used for correlation analysis. Again, the interval with the highest correlation number is introduced as the region of the expected event. However, if the highest correlation number for an isolated cluster is less than 0.8, a search is carried out for finding a high population cluster which has a similar length with it. The locations of the P- and T-waves of an isolated cluster are estimated based on the associated locations of the high population cluster.

2.4. Random walks noise theory and its application in changing the quality of artificial ECG signals

For generation of a suitable synthetic ECG database, two crucial items should be considered. First, the waveshape of the incorporated

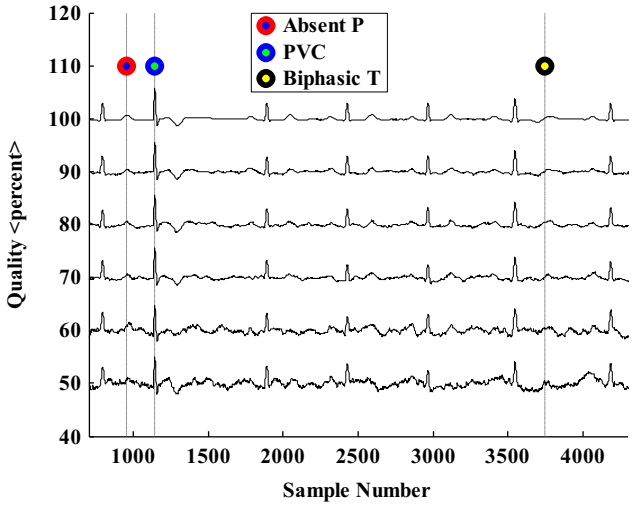

Fig. 9. Changing arbitrarily the quality of a clean ECG signal from 100 to 50% by regulating the RW noise parameter.

events should be sufficiently similar to the real forms of the ECG waves. Second, changing arbitrarily the quality of the generated ECG signal by means of a suitable disturbing potential (which simulates accurately noise effects) should be feasible. In some studies, the noise effects are modeled by periodic function, Gaussian noise, 50 Hz disturbances, white and colored noise, and some other approaches [32]. However, empirical assessments show that the real noise of the ECG signal (either ambulatory or supine), is not similar to these models. Hence, these introduced approaches do not cover all real uncertainties caused by the ECG noises. In the study [18], a suitable noise model established based on the random walks (RW) theory is proposed. This contamination model does not have a specific frequency distribution. Also, the RW has the infinity standard deviation in high number of random walks. In the study [18], the signal quality versus the random walks parameter α has been obtained numerically which gives a guideline for changing arbitrarily the quality of a clean signal from 1 (the best) to 0 (the worst) quality. More details about the proposed technique and associated mathematical materials are left to be seen in that paper.

2.5. Synthetic ECG generation

In the previous studies, a mathematical model was described and developed based on a set of algebraic equations which is capable for generating artificially normal events of the ECG such as P-wave, QRS complex, and T-wave [20,21]. The generated ECG signal simulates different real conditions such as PVCs, P-wave absence and biphasic T-waves. In addition, the RW noise source with varying magnitude is simulated in order to be added to the generated ECGs. In Fig. 9, a synthetic ECG signal which contains biphasic T-waves, PVC and P-absent beats, is shown in different quality values.

3. Results and discussions

3.1. Computerized implementation of the proposed method

Implementation of the described algorithm was done by application of the C++ platform. The developed program is capable for plotting ECG signal including the annotated events (P, Q, R, S and T). This program reads the input signal from a MAT-File (.mat). It uses MATLAB C MAT-File APIs for reading/writing a MAT compatible file. This implementation method enables a regular desktop computer to run the program successfully.

Table 1
Comparison of the detection performance of the proposed method with the most significant previous works making use of QTDB.

Method	Accuracy parameters	P_{ON}	P_{OFF}	R	T_{ON}	T_{OFF}
This study	Se (%)	99.97	99.97	99.97	99.97	99.97
	P+ (%)	99.99	99.99	99.99	99.99	99.99
Madeiro et al. [10]	Se (%)	99.32	99.32	99.32	99.32	99.32
	P+ (%)	99.47	99.47	99.47	99.47	99.47
Martínez et al. [6]	Se (%)	99.20	99.20	99.20	99.20	99.20
	P+ (%)	99.01	99.01	99.01	99.01	99.01
Ghaffari et al. [15]	Se (%)	99.64	99.64	99.97	99.93	99.93
	P+ (%)	99.00	99.00	99.95	99.92	99.92
Martínez et al. [16]	Se (%)	98.87	98.75	NR	NR	99.77
	P+ (%)	91.03	91.03	NR	NR	97.79
Laguna et al. [8]	Se (%)	97.7	97.7	NR	NR	99.0
	P+ (%)	91.17	91.17	NR	NR	97.71
Vila et al. [33]	Se (%)	NA	NA	NR	NR	92.6
	P+ (%)	NA	NA	NR	NR	NR

(Se, Sensitivity, P+: Positive Predictive Value, NA: not applicable, NR: not reported).

Table 2
Performance evaluation of several P and T detection algorithms: application to MITDB.

Detection algorithm	TP	FP	FN	Error (%)	Se (%)	P+ (%)
This study	109,381	70	39	0.09	99.96	99.94
Homaeinezhad et al. [12]	109,375	81	53	0.12	99.95	99.93
Ghaffari et al. [13]	109,367	89	61	0.14	99.94	99.91
Martinez et al. [16]	109,208	153	220	0.34	99.80	99.86
Li et al. [11]	104,070	65	112	0.17	99.89	99.94
Hamilton et al. [7]	108,927	248	340	0.54	99.69	99.77

3.2. Performance evaluation of the proposed method

According to what presented in the introduction section, several in-depth researches have been undertaken in the area of P- and T-waves detection and delineation. In many of them, the validation stage is fulfilled by applying the proposed algorithms to the QTDB and MITDB. Although the reported accuracy of some researches is about 100%, apparently, achieving such accuracy is totally dependent upon the overall quality of the ECG signal. Therefore, in this study, the performance of the proposed method is evaluated versus different signal quality values. However, in order to provide results compared with some other proposed methods, the accuracy of the presented algorithm is also assessed using the mentioned databases. The result of this assessment can be seen in Tables 1 and 2 for the QTDB and the MITDB, respectively.

3.3. Synthetic ECG recordings

As it is shown in Fig. 10(a), the percentage of isolated clusters (Section 2.4) increases together with the decrement in signal quality value. In other words, the more the signal quality value is reduced, the more number of intrinsically similar RR cycles are broken up into individual clusters. It can be seen that by decreasing the quality value to less than 60%, almost every two consecutive R-waves generate an individual cluster, (Fig. 10(a)). According to the explanations of Section 2.4, in noisy conditions, an isolated cluster usually causes the replacement of the correlation analysis by the location guess procedure. Consequently, the

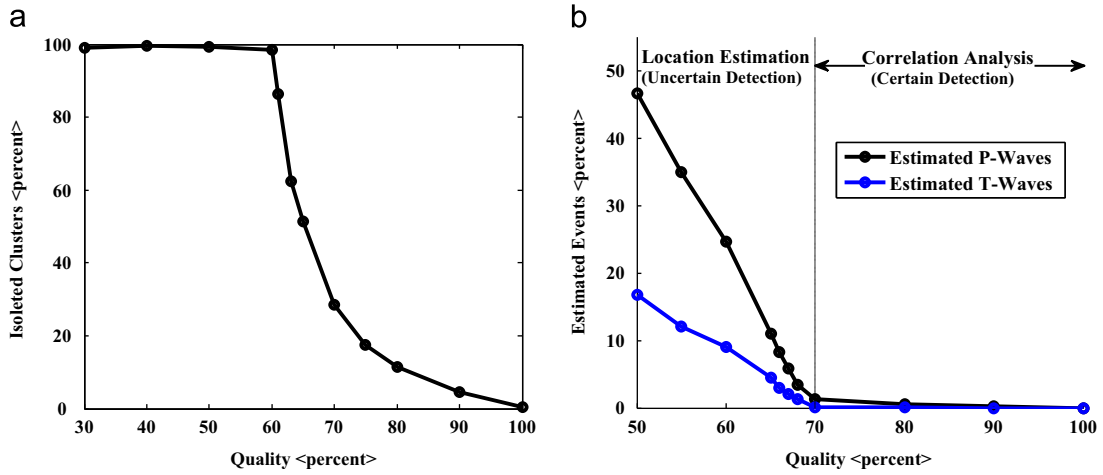

Fig. 10. Illustration of the relationship between signal quality value and (a) percentage of isolated clusters and (b) percentage of estimated events.

Table 3
The percentage of the events identified by estimation along with the delineation error of the detected ECG events versus different signal quality values.

Quality (%)	Accuracy parameter	P_{ON}	P_{OFF}	R	T_{ON}	T_{OFF}
100	Estimated (%)	0	0	0	0	0
	RMSE (s)	0.0381	0.0273	0.0028	0.0334	0.0308
90	Estimated (%)	0.17	0.17	0	0	0
	RMSE (s)	0.0373	0.0293	0.0029	0.0624	0.0430
80	Estimated (%)	0.55	0. 55	0	0.04	0.04
	RMSE (s)	0.0394	0.0248	0.0029	0.0403	0.0426
70	Estimated (%)	1.26	1.26	0	0.1	0.1
	RMSE (s)	0.0391	0.0294	0.0029	0.0327	0.0405
60	Estimated (%)	25.65	25.65	0	9.48	9.48
	RMSE (s)	0.0512	0.0405	0.0030	0.0618	0.0654
50	Estimated (%)	46.56	46.56	0	16.81	16.81
	RMSE (s)	0.0492	0.0428	0.0032	0.0658	0.0678

decrement in the signal quality value results in using location guess procedure more frequently. This fact is illustrated by Fig. 10 (b). Two major points can be observed in Fig. 1. The estimation (location guess) percentages associated with P- and T-waves are considerably different which is because of lower strength of P-waves against noises and artifacts, 2. The use of estimation suddenly increases for signal qualities less than 70%. This behavior implies that a crisp boundary can be found between guessing and certain detection of P- and T-waves.

In this study, the FP error (marking present P-waves as absent) and FN error (marking absent P-waves as present) of P-wave absence identification in RR cycles is assessed to beabout zero for correctly detected QRS complexes. Since the P- and T-wave detection phase is established on the QRS complex detection and delineation stage, a direct relationship exists between QRS detection accuracy and P- and T-wave detection precision rates. The overall accuracy of the proposed algorithm obtained by its application to synthetically generated ECG signals is presented in Table 3 versus different quality values. Each generated signal contains 500 beats sampled at the rate of 250 Hz. In these artificial ECG signals, several conditions such as absent P-wave, PVCs (premature ventricular contraction) and biphasic T-waves are incorporated, (Fig. 9).

According to the fact that performance of the cluster analysis in signals with quality values less than 70% is not reliable, the detection of P- and T-waves is not possible. Hence, for assessing the operating characteristics of the proposed algorithm in quality values less than 70%, a few beats with higher quality values were generated and then inserted into the low quality ECG signals.

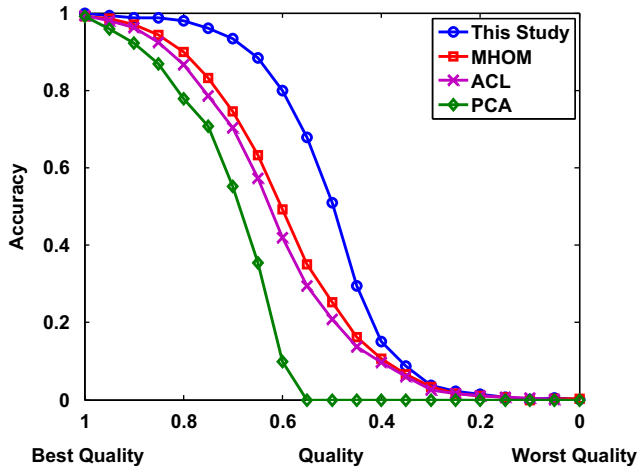

Fig. 11. A comparison between different techniques to render the non-impulsive variation of P- and T-detection accuracy versus several quality values.

3.4. Noise robustness analysis of proposed algorithm: comparative assessment

Finally, for showing the superiority of the proposed algorithm relative to the conventional wave detection techniques, a synthetic ECG database is generated. The quality of this database is altered from the best (quality=1.0) to the worst (quality=0.0) cases according to the technique introduced in Section 2.4. During each decrement of the quality, the accuracy of the detection algorithm proposed in the presented study is compared with the multiple higher order moments (MHOM) [25], area curve length (ACL) [15], and wavelet-based principal components analyzed (PCA) [12] techniques. In Fig. 11, the accuracies of the tested algorithms for detection of P- and T-waves are depicted versus the quality value variable. As it can be seen in Fig. 11, in high qualities, all algorithms give acceptable results. However, parallel to decrement of the database quality, the operation characteristics of the algorithms differ from each other which show the robustness extent of each algorithm. For example, in quality about 0.6, the accuracy of the proposed technique, MHOM, ACL, and PCA are about 81%, 64%, 59%, and 11% respectively. thanks to the use of the proposed pattern recognition and template extraction techniques, It can be concluded that the robustness of the proposed algorithm versus noise potentials is increased significantly.

4. Conclusions

In this study, a procedure for detecting and delineating non-impulsive events of the ECG signal was described. The major step of this study is a pattern recognition algorithm designed for distinguishing various ECG clusters which take place between consecutive R-waves. The performance characteristics of the proposed P and T detection–delineation algorithm were evaluated versus various ECG signals whose qualities were altered based on the random-walk noise theory. The conducted evaluations indicate that in a signal with low quality value (about 60%), the proposed method detects P and T waves with sensitivity Se=85% and positive predictive value of P+=89%, respectively. At the same quality, the average delineation errors associated with those ECG events are 45 and 63 ms, respectively. Stable delineation error, high detection accuracy and high noise tolerance were the most important aspects considered during development of the proposed method.

Conflict of interest statement

None declared.

Funding

None.

Ethical approval

Not required.

Appendix

List of variables and parameters

$2WL+1$	analysis window length
$S[n]$	original ECG signal sequence
RR_k	time distance between the k-th and $(k+1)$th R-waves
$RR_k[n]$	waveform between the k-th and $(k+1)$th R-waves
τ_V	maximum acceptable distance between $V_{RR}[n]$ and $\overline{V}_{RR}$
$\overline{V}_{RR}$	mean value of the $V_{RR}[n]$ sequence
Q_F^*	fiducial point of a cluster center
S_J^*	J-point of a cluster center
$G[n]$	trigonometric curve used for detecting P- and T-waves onset and offset
$\overline{V}_{RS}$	mean value of the $V_{RS}[i]$ sequence
E_i^C	the i-th local extremum on a cluster center waveform
RR_{Min}	minimum value of RR_k
RR_{Mean}	mean value of RR_k
RR_{ct}	the RR interval criterion; used for secondary QRS detection in order to minimize FN error
C_i	the i-th cluster of RR cycles
$C_i[n]$	waveform of the i-th cluster center
τ_D	maximum acceptable time difference between a cluster center and the test cycle
$RR_k^*[n]$	waveform between the k-th and $(k+1)$th R-waves with a DC value of zero
$V_{RR}[n]$	difference between $RR_i^*[n]$ and $C_j[n]$
τ_R	maximum acceptable value for $\overline{V}_{RR}$
τ_W	time duration threshold for the deviation of $V_{RR}[n]$ from $\overline{V}_{RR}$

References

[1] H. Naseri, M.R. Homaeinezhad, H. Pourkhajeh, Noise/spike detection in phonocardiogram signal as a cyclic random process with non-stationary period interval, Comput. Biol. Med. 43 (9) (2013) 1205–1213.

[2] J.P.V. Madeiro, P.C. Cortez, J.a.L. Marques, C.R.V. Seisdedos, C.R.M.R. Sobrinho, An innovative approach of QRS segmentation based on first-derivative, Hilbert and Wavelet Transforms, Med. Eng. Phys. 34 (9) (2012) 1236–1246.

[3] L.G. Tereshchenko, L. Han, A. Cheng, J.E. Marine, D.D. Spragg, S. Sinha, D. Dalal, H. Calkins, G.F. Tomaselli, R.D. Berger, Beat-to-beat three-dimensional ECG variability predicts ventricular arrhythmia in ICD recipients, Heart Rhythm 7 (11) (2010) 1606–1613.

[4] C. Teodorescu, K. Reinier, A. Uy-Evanado, J. Navarro, R. Mariani, K. Gunson, J. Jui, S.S. Chugh, Prolonged QRS duration on the resting ECG is associated with sudden death risk in coronary disease, independent of prolonged ventricular repolarization, Heart Rhythm: Off. J. Heart Rhythm Soc. 8 (10) (2011) 1562–1567.

[5] M.L. Bertoia, M.a Allison, J.E. Manson, M.S. Freiberg, L.H. Kuller, A.J. Solomon, M.C. Limacher, K.C. Johnson, J.D. Curb, S. Wassertheil-Smoller, C.B. Eaton, Risk factors for sudden cardiac death in post-menopausal women, J. Am. Coll. Cardiol. 60 (25) (2012) 2674–2682.

[6] A. Martínez, R. Alcaraz, J. Rieta, Application of the phasor transform for automatic delineation of single-lead ECG fiducial points, Physiol. Meas. 31 (11) (2010) 1467–1485.

[7] P. Hamilton, W. Tompkins, Quantitative investigation of QRS detection rules using the MIT/BIH arrhythmia database, IEEE Trans. Biomed. Eng. 33 (1986) 1157–1165.

[8] P. Laguna, R. Jané, P. Caminal, Automatic detection of wave boundaries in multilead ECG signals: validation with the CSE database, Comput. Biomed. Res. 27 (1) (1994) 45–60.

[9] H.K. Chatterjee, R. Gupta, M. Mitra, Real time P and T wave detection from Ecg using Fpga, Procedia Technol. 4 (2012) 840–844.

[10] J.P.V Madeiro, W.B. Nicolson, P.C. Cortez, J.A.L. Marques, C.R. Vázquez-Seisdedos, N. Elangovan, G.A. Ng, F.S. Schlindwein, New approach for T-wave peak detection and T-wave end location in 12-lead paced ECG signals based on a mathematical model, Med. Eng. Phys. 35 (8) (2012) 1105–1115.

[11] C. Li, C. Zheng, C. Tai, Detection of ECG characteristic points using wavelet transforms, IEEE Trans. Biomed. Eng. 42 (1995) 21–28.

[12] M.R. Homaeinezhad, A. Ghaffari, H.N. Toosi, M. Tahmasebi, M.M. Daevaeiha, Optimal delineation of ambulatory Holter ECG events via false-alarm bounded segmentation of a wavelet-based principal components analyzed decision statistic, Cardiovasc. Eng. 10 (2010) 136–156.

[13] A. Ghaffari, M.R. Homaeinezhad, M.M. Daevaeiha, High resolution ambulatory holter ECG events detection–delineation via modified multi-lead wavelet-based features analysis: detection and quantification of heart rate turbulence, Expert Syst. Appl. 38 (5) (2011) 5299–5310.

[14] S. Pal, M. Mitra, Detection of ECG characteristic points using Multiresolution Wavelet Analysis based Selective Coefficient Method, Measurement . 43 (2) (2010) 255–261.

[15] A. Ghaffari, M.R. Homaeinezhad, M. Akraminia, M. Atarod, M. Daevaeiha, A robust wavelet-based multi-lead electrocardiogram delineation algorithm, Med. Eng. Phys. 31 (10) (2009) 1219–1227.

[16] J.P. Martínez, R. Almeida, S. Olmos, A.P. Rocha, P. Laguna, A wavelet-based ECG delineator: evaluation on standard databases, IEEE Trans. Bio-med. Eng. 51 (4) (2004) 570–581.

[17] S.S. Mehta, N.S. Lingayat, Application of support vector machine for the detection of P- and T-waves in 12-lead electrocardiogram, Comput. Methods Programs Biomed. 93 (1) (2009) 46–60.

[18] H. Naseri, H. Pourkhajeh, M.R. Homaeinezhad, A unified procedure for detecting, quantifying, and validating electrocardiogram T-wave alternans, Med. Biol. Eng. Comput. 51 (9) (2013) 1031–1042.

[19] H. Naseri, M.R. Homaeinezhad, H. Pourkhajeh, An expert electrocardiogram quality evaluation algorithm based on signal mobility factors, Med. Eng. Technol. 37 (4) (2013) 282–291.

[20] A. Ghaffari, M.R. Homaeinezhad, Y. Ahmadi, An open-source applied simulation framework for performance evaluation of QRS complex detectors, Simulation Modelling Pract. Theory 18 (6) (2010) 860–880.

[21] M.R. Homaeinezhad, P. Sabetian, A. Feizollahi, A. Ghaffari, R. Rahmani, Parametric modelling of cardiac system multiple measurement signals: an open-source computer framework for performance evaluation of ECG, PCG and ABP event detectors, J. Med. Eng. Technol. 36 (2) (2012) 117–134.

[22] A.L. Goldberger, L.A.N. Amaral, L. Glass, J.M. Hausdorff, P.C. Ivanov, R.G. Mark, J. E. Mietus, G.B. Moody, C.-K. Peng, H.E. Stanley, PhysioBank, PhysioToolkit, and PhysioNet: components of a new research resource for complex physiologic signals, Circulation 101 (23) (2000) e215–e220.

[23] P. Laguna, R.G. Mar, A. Goldberg, G.B. Moody, A database for evaluation of algorithms for measurement of QT and other waveform intervals in the ECG, Comput. Cardiol. 24 (1997) 673–676.

[24] G.B. Moody, R.G. Mark, The impact of the MIT-BIH arrhythmia database, IEEE Eng. Med. Biol. Mag.: Q. Mag. Eng. Med. Biol. Soc. 20 (3) (2001) 45–50.

[25] A. Ghaffari, M.R. Homaeinezhad, M. Khazraee, M.M. Daevaeiha, Segmentation of holter ECG waves via analysis of a discrete wavelet-derived multiple skewness–kurtosis based metric, Ann. Biomed. Eng. 38 (4) (2010) 1497–1510.

[26] E.J. Ciaccio, A.B. Biviano, W. Whang, J. Coromilas, H. Garan, A new transform for the analysis of complex fractionated atrial electrograms, Biomed. Eng. Online 10 (1) (2011) 35.

[27] E.J. Ciaccio, A.B. Biviano, W. Whang, A.L. Wit, J. Coromilas, H. Garan, Optimized measurement of activation rate at left atrial sites with complex fractionated electrograms during atrial fibrillation,, J. Cardiovasc. Electrophysiol. 21 (2) (2010) 133–143.

[28] E.J. Ciaccio, A.B. Biviano, W. Whang, H. Garan, J. Coromilas, New methods for estimating local electrical activation rate during atrial fibrillation, Heart Rhythm 6 (1) (2009) 21–32.
[29] T. Li, T.P. Sattar, S. Sun, Deterministic resampling: unbiased sampling to avoid sample impoverishment in particle filters, Signal Process. 92 (7) (2012) 1637–1645.
[30] J. McBride, A. Sullivan, H. Xia, A. Petrie, X. Zhao, Reconstruction of physiological signals using iterative retraining and accumulated averaging of neural network models, Physiol. Meas. 32 (6) (2011) 661–675.
[31] G.B. Moody, The physionet/computing in cardiology challenge 2010: mind the gap, Comput. Cardiol. 37 (2010) 305–309.
[32] B. Ghoraani, S. Krishnan, R.J. Selvaraj, V.S. Chauhan, T wave alternans evaluation using adaptive time-frequency signal analysis and non-negative matrix factorization, Med. Eng. Phys. 33 (6) (2011) 700–711.
[33] J.A. Vila, Y. Gang, J.M. Rodriguez Presedo, M. Fernández-Delgado, S. Barro, M. Malik, A new approach for TU complex characterization, IEEE Trans. Bio-med. Eng. 47 (6) (2000) 764–772.